論文 94-19-11-3

Hough Transform Based Projection Method for Target Tracking in Image Suquences

Jae Ho Choi* Hoon Sung Kwak*, *Regular Members*

투사 및 허프 변환 방식에 의한 연속 영상상의 비행체 궤적 추적

正會員 崔 在 虎* 正會員 郭 勳 星*

요 약

본 논문은 레이돈(Radon) 변환식으로부터 유도된 투사 근거 허프(Hough) 변환 방식을 사용하여 시간연속 영상상의 이동물체의 궤적을 추정하는 기법을 제안한다. 이때 이동비행물체는 시간연속되는 각 영상 프레임에 몇 개의 화소로 나타나며 그 궤적은 삼차원 직선으로 간주한다. 근래에 제시된 방법들은 합성영상 인단일 궤적도면을 여러 종류의 허프 변환 방식을 사용하여 그 궤적을 추정하여 왔으나 본 논문의 방식은 시간연속 영상을 여러 방향에서 투사하여 얻어지는 이차원적 비행체 궤적 지식을 효과적으로 비행체 궤적 재구성에 이용함으로 비행체 탐지 능력은 물론 궤적 추정 능력을 향상하였다. 아울러 투사 근거 허프 변환방식을 평가, 사정하기 위하여 영상 공간의 소음등으로 야기된 투사 공간상의 허프 파라미터의 추정 error를 분석, 유도하였다. HiCamps라 명칭된 실제 적외선 시간연속 영상 데이타를 대상으로 시뮬레이션한 결과 비행체 궤적 추정이 아주 낮은 SNR 에서도 가능함을 보여준다.

ABSTRACT

This paper contains a Hough transform based projection method derived from Radon transform for tracking dim, unresolved(sub pixel) moving targets that move along straight line paths across a time sequential image data. In contrast to several recently presented Hough transform methods using a compressed image referred to as the track map, our proposed technique utilizing a set of projections taken along arbitrary orientations effectively increases the chances of target detection, and creates a robust track estimation environment by incorporating all the available knowledge obtained from the projections. Moreover, in order to quantitatively assess the estimation capability of the projection-based Hough transform algorithm, the analytical bounds on the Hough space parameter errors introduced by image space noise contamination are derived. The simulation yielded promising results of estimating the track parameters even under low signal to noise ratios when our technique was tested against the time sequential sets of real infrared image data referred to as the HiCamps.

* 전북대학교 컴퓨터 공학과
Department of Computer Engineering Chonbuk National University
論文番號 : 93217
接受日字 : 1993年 11月 11日

Ⅰ. INTRODUCTION

In 1962, Hough[1] introduced a method for detecting complex patterns of points in binary image data by determining specific values of parameters characterizing these patterns. Since then, the Hough transform has been extended to estimate the parameters of straight lines and curves in gray scale images[2][3] and to extract the primitive geometric shapes[4][5].

One application area in which the Hough transform methodology has been successfully applied is the detection and estimation of point target tracks.

Cowart et al.[6] applied a traditional straight-line finding Hough transform algorithm to detect non maneuvering target trajectories. Later, Padgett at al.[7] extented the Cowart et al. 's method to allow for the detection of maneuvering circular target tracks. Alternativerly, Casasent et al.[8] developed a technique using a modified Hough transform to estimate the parameters of elliptical target trajectories. These techniques have a similarity in that the Hough transform was applied to a two-dimensional compressed image data called a track map. Unfortunately, if the unresolve targets are dim and buried in backgroud clutter, the performance of aforementioned Hough transform algorithms degrades fast. Even when preprocessing is performed to help reduce the amount of clutter in the data, there is still a limit to one's ability to detect dim, unresolved targets(target spatial extent less than a pixel) in cluttered backgrounds if the original data has been projected only along the temporal axis to obtain the track map.

The problem addressed in this paper is the robust detection and estimation of non-maneuvering target track parameters using a three-dimensional volume of data composed of the time-sequential set of image frames. The three dimensions of the data include two spatial dimensions and one temporal dimension. The proposed solution uses a projection-based Hough transform method derived from Radon transform[9]. In the general case, the Radon transform produces a set of (N-1)-dimensional projections from an N-dimensional function. Computing the Radon transform consists of computing the projections of image data along a particular pattern, e.g., a straight line or plane. Although there is an increase in the number of computations needed to compute a set of projections, there is also an increase in ability to distinguish tracks at various orientations.

For the rest of paper, the newly proposed generalized projection-based Hough transform methhod is described in Section II. In Section III the analytical derivation for the estimated Hough parameter errors introduced by the image space noise contamination is presented. The simulation results and the conclusions are in Section IV and V, respectively.

Ⅱ. HOUGH TRANSFORM BASED PROJECTION METHOD

In this section, a generalized projection based Hough transform method derived from Radon transform is presented. The Radon transform provides a mean to obtain a set of 2-D projections from a 3-D volume of image data. By analyzing the 2-D multiple views of the 3-D track volume a robust set of track parameters can be generated, even under noisy conditions.

Computing the Radon tranform consists of computing the projections of an image along a particular pattern, e.g., a straight line. For the 2-D

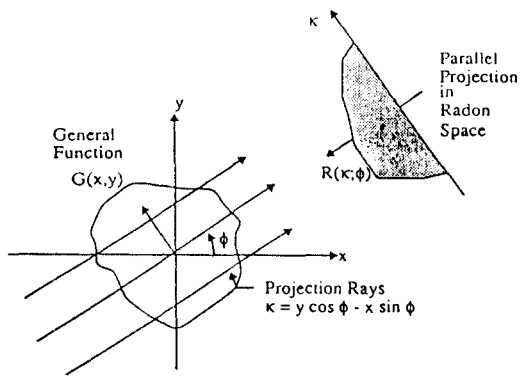

Figire 1. Geometry for the two-dimensional Radon transform.

Radon transform, consider a two dimensional function G(x,y) as shown in Fig.1.

The integral of G(x,y) along a projection ray is called a ray integral, and a set of ray integrals forms a projection. The equation for the individual ray is given by

$$k = y\cos\phi - x\sin\phi \tag{1}$$

where k is the perpendicular distance of the projection ray from the origin.

The integral function of G(x,y) along the ray can be expressed as follows:

$$P(k,\phi) = \int\int G(x,y)\,\delta (x - y\cos\phi + x\sin\phi)\,dxdy \tag{2}$$

where P(k,ϕ) as a function of k is the paralled projection of G(x,y) for angle ϕ, and δ is the convolving kernel defined by Eq(1). The whole distribution of projections forms the Radon transform of G(x,y).

Eq.(2) can be extended to a three dimensional Radon transform as follows:

$$P(k,\tau,\phi) = \int\int\int T(x,y,t) \cdot \delta(k - y\cos\phi + x\sin\phi,\ \tau - t) \cdot dxdydt \tag{3}$$

The two dimensional function P(k,τ,ϕ) as a function of κ and τ is the surface integral of a volume T(x,y,t) over the projection plane for angle ϕ. The whole three dimensional distribution of the paralled projections forms a three dimensional Radon transform of T(x,y,t).

In the actual implementation, however, instead of the convolution along the projection angle, the maximum value finding scheme is incorporated. In[10] the performance of the optimal projection method is compared to the maximum value projection and the summation projection method. It was shown that the maximum value projection is as nearly good as the optimal projection and requires fewer computations. Hence, our generralized projection based transform method modifying the 3-D Radon transform can be defined as follows:

$$M(k,t,\phi) = Maximum[\ (x,y,t) \mid k - y\cos\phi + x\sin\phi = 0, (x,y,t) \in T(x,y,t)] \tag{4}$$

The visualization for taking a set of projections of the 3-D volume of data composed of the time sequential set of imageries using our generalized projection based transform method is shown in Fig. 2.

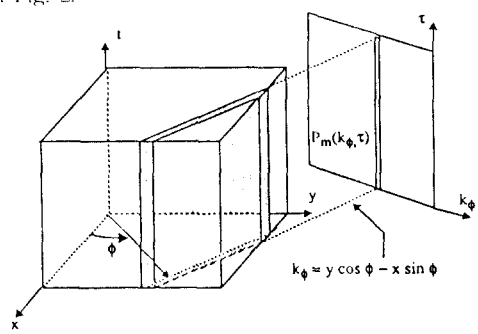

Figure 2. Geometry of the modified three-dimensional Radon transform.

Furthermore, since the volume T(x,y,t) can be viewed along another unique orientation, we may define another projection plane as follows:

$$l = t\cos\phi - y\sin\phi \tag{5}$$

and by taking paralled projections using Eq.(5), another unique set of projections can be obtained as follows:

$$M(l,x,\phi) = Maximum[\ (x,y,t) \mid \cdot\ l - t\cos\phi + y\sin\phi = 0, (x,y,t) \in T(x,y,t)] \tag{6}$$

Theoretically, incresaing the number of projections

improve the performance of the estimation, but increases the cost of computation.

Supposing the number of projections taken along ψ orientation is four, then the projection frames would be taken along which ψ equals o, 30, 60, and 90 degrees increamenting the projection angle ψ by thirty degrees at each time.

Once two sets of projection frames are obtained using Eq.(4) and (6), the target track parameters are estimated through the straight-line finding 2-D Hough transform as shown in Fig. 3.

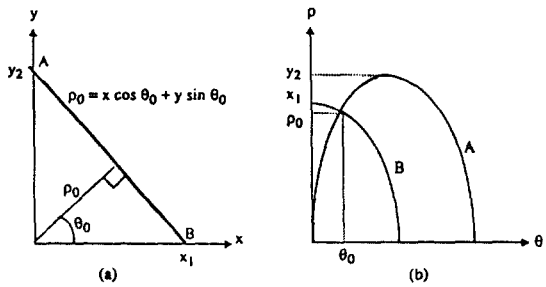

Figure 3. Mappaing in 2-D Hough transform : Points A and B are mapped to curves A and B in Hough parameter space (ρ, θ). The line in (a) maps to a point. (ρ_o, θ_o) in (b).

The estimated track parameters for two sets of the paralled projection frames are denoted as $(\overline{\rho}_i, \overline{\theta}_i)$ for i = 1, 2,...,C1, and $(\overline{\rho}_j, \overline{\theta}_j)$ for j = 1, 2,..., CJ, respectively. Here, $\overline{\rho}_k$ and $\overline{\theta}_k$ represent the estimated normal distance between the projected track and the origin of the kth projection space, and the estimated angle between the normal line and the x_k-axis of the kth projection space, respectively.

In order to reconstruct the estimated target track back in the original 3-D image space, a back-projection along its corresponding reverse direction is performed as follows:

$$\begin{aligned}&\overline{T}(x,y,t)\\&=\bigcap_{i=1}^{C_1}[\ (x,y,t)\mid k-y\cos\phi+x\sin\phi\\&=0,(k.t,\phi)\in\overline{T_i}(k,t,\phi)]\\&+\bigcap_{j=1}^{C_j}[\ (x,y,t)\mid l-t\cos\phi+y\sin\phi\\&=0,(l,x,\psi i)\in\overline{T_j}(l,x,\psi i)]\end{aligned}\tag{7}$$

where $\overline{T}$(x,y,t) is the intersection of all those feature points estimated and back-projected from each set of projection spaces onto the original image space and $\overline{T_i}$(k,t,ψ) and $\overline{T_j}$(l,x,ψ), respectively, are the estimated 2-D target tracks for two sets of projections using the inverse Hough transform as follows:

$$\overline{T_j}(k,t,\phi)=\begin{cases}1, & \text{for } \overline{\rho}_i-k\cos\overline{\theta}_i-t\sin\overline{\theta}_i=0\\0, & otherwise\end{cases}\tag{8}$$

and

$$\overline{T_j}(l,x,\psi)=\begin{cases}1, & \text{for } \overline{\rho}_j-l\cos\overline{\theta}_i-x\sin\overline{\theta}_j=0\\0, & otherwise\end{cases}\tag{9}$$

The convergence of the track estimation problem is limited by the input image frame signal-to-noise ratio and the dicretization errors in projections. The projection error occurs when the data is recorded discretely and when there is a projection onto a plane that is not parallel to one of the spatial or temporal directions. As an assessment for the projection-based Hough transform algorithm, the analytical error bounds on the estimated Hough space parameters induced by the image space noise contamination is derived in the next section.

Ⅲ. ANALYTICAL ERROR BOUNDS ON HOUGH PARAMETERS

In the projection-based transformation the system is overdatermined by taking arbitrary number of projections along the projection orientations defined

by the hyperplanes k and l. The target movement is assumed to be non-maneuvering with the minimal acceleration and deceleration for the time duration of the problem investigation, and the target speed is set to one pixel per frame. Hence, the traditional straight-line finding 2-D Hough transform is applied to each one of the projection frames in order to estimate the target track parameters ρ_k and θ_k in each one of the corresponding Hough parameter spaces. These set of Hough parameters are used to composed 2-D tracks back in the projection spaces using the inverse Hough transform; and those 2-D tracks are back projected onto the original 3-D image space to reconstruct the target trajectory. When the original 3-D volume of the time sequential image data is noiseless the tracking problem becomes trivial, and the system produces the accurate set of target track parameter estimates, ρ and θ. These parameters along with time information defines the directional motion of the target with a speed of 1 pixel/frame. However, in noisy case, the reconstruction through back projection is made of a 3-D track volume due to estimation errors in the Hough parameters resulted from image space noise contamination.

In this section a derivation of analytical bounds on the Hough space parameter errors that are introduced by image space noise contamination is presented. This will provide a mechanism for quantitatively assessing track estimation performance of the generalized projection based Hough transform algorithm.

Conider that a 3-D volume of image data is generated from a time sequence of 2-D image frames. A set of 2-D projection data is then obtained from the 3-D volume as in eq. (4) and (6). A straight-line target track in a 2-D projection space is modeled by

$$\rho_i = x_i \cos\theta_i + y_i \sin\theta_i \tag{10}$$

where xi and yi are the spatial coordinates for an arbitrary 2-D projection space and ρ_i and θ_i and the corresponding Hough space parameters. If the data is noisy, there will be errors in the estimates of the Hough space parameters. We are interested in determining the bounds on the errors for the estimated ρ_i and θ_i.

An error in the estimate of the Hough space parameters ρ_i and θ_i will result in an error in the estimated target track. An estimated target track will fall within some neighborhood (noise strip) of the actual target track location as shown in Fig. 4. Here, without the loss of generality the sampling grid is assumed to be rectangular in the projection-space spatial plane with the pixed dimensions given by Δxi and Δyi.

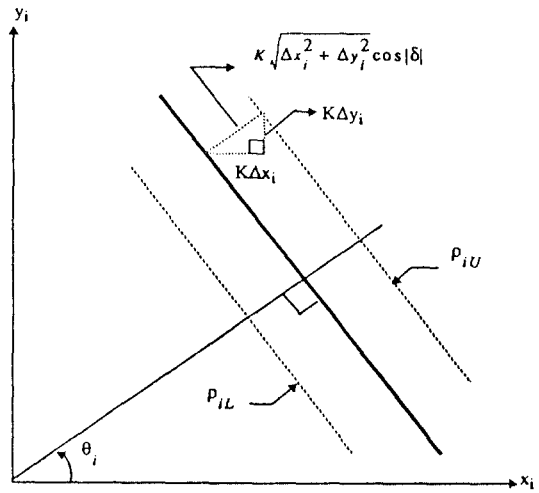

Figure 4. Geometry associated with determining error bounds on $\overline{\rho_i}$ and $\overline{\theta_i}$ of the target track.

The estimate of an actual target point location (xi,yi) is given by

$$\overline{x_i} = x_i + \varepsilon_1 \tag{11}$$

$$\overline{y_i} = y_i + \varepsilon_2 \tag{12}$$

where ε_1 and ε_2 are assumed to be an i.i.d. (independtly, identically distributed) zero mean moise. Suppose

$$|\varepsilon_1| \le K\Delta x_i \tag{13}$$

$$|\varepsilon_2| \le K\Delta y_i \tag{14}$$

where K is a constant. For these cases, the estimated track points could lie as far as away from the actual track point. In general, the amount of error will depend on the discretization noises (quantization and sampling errors) and location of the track.

1. Error Bounds on estimatess of ρ_i

1.1 For $0 \le \theta_i \le \pi/2$

A bound on the estimate of ρ_i can be specified as a function of θ_i as follows:

$$(x_i - K\Delta X_i)\cos\theta_i + (y_i - K\Delta y_i)\sin\theta_i \le \overline{\rho_i}$$
$$\overline{\rho_i} \le (x_i + K\Delta x_i)\cos\theta_i + (y_i + K\Delta y_i)\sin\theta_i \tag{15}$$

where $\overline{\rho_i}$ is the estimate of ρ_i

Consider the problem geometry shown in Fig. 4. Here,

$\rho_i U$ = upper bound of estimate

$\rho_i L$ = lower bound of estimate

The upper and lower bound on the estimate of pi is derived as follows:

$$\rho_{iU} = (x_i + K\Delta x_i)\cos\theta_i + (y_i + K\Delta y_i)\sin\theta_i \tag{16}$$

$$\rho_{iL} = (x_i - K\Delta x_i)\cos\theta_i + (y_i - K\Delta y_i)\sin\theta_i \tag{17}$$

and

$$\rho_{iL} \le \overline{\rho_i} \le \rho_{iU} \tag{18}$$

where

$$\overline{\rho_i} = (x_i + \varepsilon_1)\cos\theta_i + (y_i + \varepsilon_2)\sin\theta_i \tag{19}$$

Then,

$$|\Delta\rho_i| = |\rho_i - \overline{\rho_i}| = \sqrt{\varepsilon_1^2 + \varepsilon_2^2}\cos|\theta_i - 45^\circ| \tag{20}$$

and

$$|\Delta\rho_i| \le |\rho_i - \rho_{iL}| = |\rho_i - \rho_{iU}| = K\sqrt{\Delta x_i^2 + \Delta y_i^2}\cos|\theta_i - 45^\circ| \tag{21}$$

1.2 For $\pi/2 < \theta_i < \pi$

$$\rho_{iU} = (x_i - K\Delta x_i)\cos\theta_i + (y_i + K\Delta y_i)\sin\theta_i \tag{22}$$

$$\rho_{iL} = (x_i + K\Delta x_i)\cos\theta_i + (y_i - K\Delta y_i)\sin\theta_i \tag{23}$$

and

$$|\Delta\rho_I| \le k\sqrt{\Delta x_I^2 + \Delta x_I^2}\cos|\theta_i - 135^\circ| \tag{24}$$

1.3. For $3\pi/2 < \theta_{i,} < 2\pi$

$$\rho_{iU} = (x_i + K\Delta x_i)\cos\theta_i + (y_i - K\Delta y_i)\sin\theta_{i,} \tag{25}$$

$$\rho_{iL} = (x_i - K\Delta x_i)\cos\theta_i + (y_i + K\Delta y_i)\sin\theta_{i,} \tag{26}$$

and

$$|\Delta\rho_i| \le K\sqrt{\Delta x_i^2 + \Delta y_i^2}\cos|\theta_i - 135^\circ| \tag{27}$$

If we assume $\Delta x_i = \Delta y_i = 1$, then

$$|\Delta\rho_i| \le K\sqrt{2}\cos|\lambda| \tag{28}$$

where,

$$\lambda = \begin{cases} \theta_i - 45^\circ & \text{for } 0 \le \theta_i \le \dfrac{\pi}{2} \\ \theta_i - 135^\circ & \text{for } \dfrac{\pi}{2} < \theta_i < \pi \\ \theta_i - 315^\circ & \text{for } \dfrac{3\pi}{2} < \theta_i < 2\pi \end{cases} \tag{29}$$

For example, if the line track is detectable in the noise strip and K = 0.5 and $0 \le Oi \le \pi/2$, the worst case error in ρ_i is (30)

$$|\Delta\rho_i| \le 0.5\sqrt{2}\cos|45^\circ - 45^\circ| = \frac{\sqrt{2}}{2} \tag{30}$$

Thus, $\overline{\rho_i}$ lies within a ± 1 pixel strip. For K = 1.0,

$$| \Delta \rho_i | \leq \sqrt{2} \tag{31}$$

and $\overline{\rho_i}$ lies within a ± 2 pixel strip.

It is to note that in this derivation the upper left corner of the projection frame is treated as the origin of the projection space coordinate system. Hence, the third quadrant region is not considered since the Hough parameters falling in this region represent the target movement backward in time.

2. Error Bounds on estimates of Oi

Assuming the length of the actual target track is L, we have derived the upper and lower estimation bounds on λ. Considering λ defined as Eq.(20), the error bound for $\overline{\theta_i}$ can be expressed as follows:

$$| \Delta \theta_i | = | \theta_i - \overline{\theta_i} | \leq | \frac{\pi}{2} - \tan^{-1} \frac{2L}{\sqrt{\varepsilon_1^2 + \varepsilon_2^2 \cos | \lambda | }} | \tag{32}$$

Again for the case where Δxi = Δyi = 1, then

$$| \Delta \theta_i | = | \frac{\pi}{2} - \tan^{-1} \frac{2L}{K\sqrt{\Delta x_i^2 + \Delta y_i^2 \cos | \lambda | }} | \tag{33}$$

$$| \Delta \theta_i | = | \frac{\pi}{2} - \tan^{-1} [\frac{\sqrt{2}L}{K \cos | \lambda | }] | \tag{34}$$

It clearly shows that the longer the track length (i.e., more target images integrated along the track path), the higher the chances of retriving more accurate Hough parameter estimates of target tracks provided that most of the target signal points fall into the bounded strip region.

IV. SIMULATION RESULTS

Simulations are run to demonstrate the performance of our projection based transform method for estimating tracks of unresolved targets. The objective of the experiments is to study the behavior of our projection based tracking system as a function of the number of projections, the signal to noise ratios, and the number of image data frames.

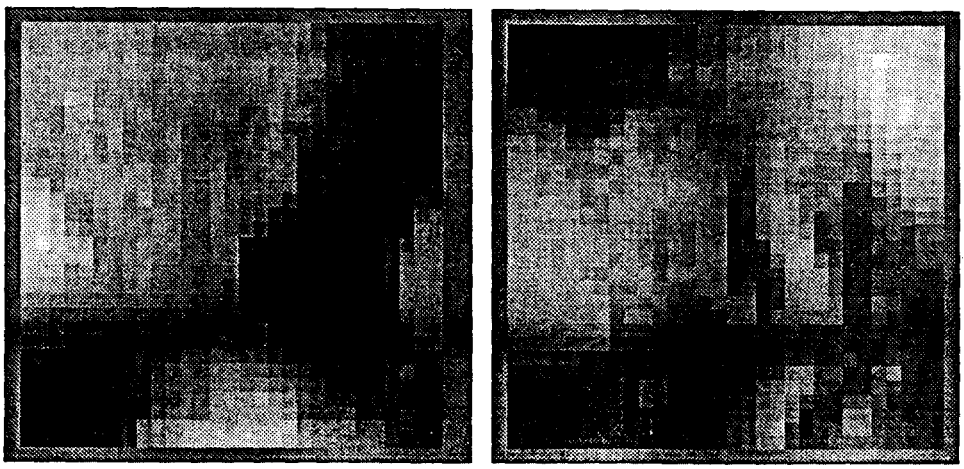

Figure 5. The images taken from the HiCamp data I(left) and II(right)

Two 8-bit real infrared image sequences made of the data called HiCamps shown in Fig. 5 were used. Each sequence has a frame size of 32 x 32 pixels and up to 46 frames in the temporal direction to accomodate the longest possible track of a target moving at a speed of one pixel per frame. Since an image sequence with a real target was not available, the target points making the target trajectory were synthetically generated and embedded into a image sequence under the assumption that a target has a spatial extent less than a pixel(sub-pixel) as follows:

$$I(x,y,t)=\begin{cases} aC+(1-a)B(x,y,t)+N, \\ \qquad \forall (x,y,t)\in T(x,y,t) \\ B(x,y,.t)+N, \\ \qquad elsewhere \end{cases} \tag{35}$$

where I(x,y,t) is the 3 D volume of time-sequential image data to be processed as an input to the tracking system, B(x,y,t) is the HiCamp image background, C Is the target signal intensity, a $(0\le a\le 1)$ is a coefficient controling the contribution of target signal to the background pixel, N is a zero mean, additive white Gaussian noise, and finally, T(x,y,t) is the target trajectory with a target speed of one pixel perframe. Eq. (35) is one of the popular infrared image model for adding the point target along the target tracjectoy. Since each data frame may contain one target point of a sup pixel size, it is practically the most reasonable to set the value of a such that the pixel location value containing the target point is made of some combination of the target and the background intensities, respectively. Here, we haver set a = 0.45 making the target signal dim with respect to the HiCamp background. For the simulation two test target tracks representing T(x,y,t) were prepared. These tarcks are denoted as Track A and Track B with the characterizing Hough parameters(ρ, θ) with respect to xy-plane at (1, 1170) and (18, 450), respectively. More extensive simulation results can be found in [11]. Furthermore, as one of the measures for the performance evaluation, the signal-to-noise ration is defined as follows:

$$SNR = 10\log_{10}\left[\frac{\sum_x\sum_y\sum_t [\,I(x,y,t)-B(x,y,t)^2}{(L\sigma_v^2)}\right], \quad \forall (x,y,t)\in T(x,y,t)$$

where L is the total number of data frames (or target points)and is the noise variance.

The goodness of etimation performance was also measured in terms of the Hough parameter estimate error bounds as follows:

1. Good setimates: when the estimated $\overline{\rho}$ resides whthin a theree pixel strip containing the true track and the estimated $\overline{\theta_i}$ is in the bound of as large as eight degrees(i.e.,K≤1.0);
2. Fair estimates: when the estimated $\overline{\rho}$ resides within a five pixel strip containing the true track and the etimated $\overline{\theta_i}$ is in the bound of as large as twelve degree (i.e., 1.0<K≤1.5);
3. Poor estimates: when the estimated $\overline{\rho}$ resides whthin a seven pixel strip containing the true track and the estimated $\overline{\theta_i}$ is in the bound of as large as sixteen degrees(i.e., 1.5<K ≤2.0);
4. Non-trackable estimates: when any of the estimated parameters $\overline{\rho}$ and $\overline{\theta_i}$ are not contained in above three.

The above measure of the error bounds assessing the performance of target tracking accuracy are determined through many simulation runs given an average of twenty data frames. Of course, the target tracking accuracy can be improved by using more data frames.

The simulation results are summarized it Tables 1 through 4 for the number of different signal-to-

noise ratuism orihectuibsm and image data frames containing a target as follows:

1. Track A in HiCamp I (Table 1): The good Track A Hough parameter estimates were obtained down to 3.6 dB given twenty or more frames of image data with as many as nine projection frames. The most of estimates were the good or fair where track parametes estimates $\overline{\rho_j}$ and $\overline{\theta_j}$ were obtained with error bounds of [0, +1] pixels and [-2, 1] degrees, respectively. The poor estimates were apparent in the very low SNR ranges;

Table 1. 2-D Hough parameter estimation of a target track Track A with true parameters(1,117°) using HiCamp image sequence I.

PROJ	Frame	Estimated 2-D Hough Parameters (ρ, θ)			
		13.0dB	8.80dB	5.90dB	3.60dB
3	15	(1,117°)	(1,118°)	(1,134°)	(1,137°)
	20	(1,117°)	(1,117°)	(1,134°)	(1,137°)
	25	(1,117°)	(1,117°)	(1,134°)	(1,137°)
6	15	(1,117°)	(1,116°)	(1,134°)	(1,137°)
	20	(1,117°)	(1,118°)	(1,134°)	(1,136°)
	25	(1,117°)	(1,118°)	(1,134°)	(1,134°)
9	15	(1,117°)	(1,116°)	(1,134°)	(2,133°)
	20	(2,117°)	(1,111°)	(1,115°)	(1,115°)
	25	(1,117°)	(1,115°)	(1,115°)	(1,115°)

2. Track B in HiCamp I (Table 2): The good Track B Hough parameter estimates were obtained down to 7.75 dB given twenty five data frames with three or more projection frames. The good or fair estimatess were observed with error bounds of [-2, +4] pixels and [-9, +11] degrees, respectively. The poor and nontrackable estimates began to show up for low SNR values;
3. Track A in HiCamp II (Table 3): The good Track A Hough parameter estimates were obtained down to 12.1 dB given twenty or more data frames with six or more projection frames. Most of good or fair estimates were observed in the medium SNR ranges with error bounds of [0, +1] pixels and [-1, +7] degrees, respectively. Some non trackable estimates appreared in the same SNR ranges for the number of projections less than six;

Talble 2. 2-D Hough parameter estimation of a target track Track B with true parameters(18,45°) using HiCamp image sequence I.

PROJ	Frame	Estimated 2-D Hough Parameters (ρ, θ)			
		13.2dB	11.9dB	8.95dB	7.75dB
3	15	(18,38°)	(8,38°)	(17,28°)	(17,28°)
	20	(18,45°)	(17,36°)	(17,28°)	(22,67°)
	25	(18,45°)	(18,45°)	(18,45°)	(18,45°)
6	15	(18,38°)	(16,36°)	(23,72°)	(23,72°)
	20	(18,45°)	(17,36°)	(22,66°)	(23,72°)
	25	(18,45°)	(18,45°)	(18,45°)	(18,45°)
9	15	(18,38°)	(16,37°)	(20,59°)	(23,378°)
	20	(18,45°)	(16,37°)	(20,59°)	(21,70°)
	25	(18,45°)	(18,45°)	(18,45°)	(18,45°)

Table 3. 2-D Hough parameter estimation of a target track Track A with true parameters(1,117°) using HiCamp image sequence II.

PROJ	Frame	Estimated 2-D Hough Paraneters (ρ, θ)			
		13.0dB	8.80dB	5.90dB	3.60dB
3	15	(1,118°)	(1,118°)	(2,342°)	(3,346°)
	20	(1,118°)	(1,118°)	(1,116°)	(3,346°)
	25	(1,118°)	(1,118°)	(1,118°)	(3,346°)
6	15	(1,118°)	(1,118°)	(1,342°)	(3,346°)
	20	(1,118°)	(1,118°)	(1,116°)	(2,124°)
	25	(1,118°)	(1,118°)	(1,116°)	(2,124°)
9	15	(1,118°)	(1,118°)	(1,342°)	(3,346°)
	20	(1,118°)	(1,118°)	(1,116°)	(1,127°)
	25	(1,118°)	(1,118°)	(1,116°)	(1,127°)

4. Track B in HiCamp II (Table 4): The good Track B Hough parameter estimates were obtained down to 5.75 dB given twenty-five frames with six projection frames or more. The

good and fair estimates were obtained down to 7.35 dBs with error bounds of [-2, +2] pixels and [0, +19] pixels, respectively. Some poor or non-trackable estimates appeared in the adverse SNR conditions with not enough data frames.

Talble 4. 2-D Hough parameter estimation of a target track Track B with true parameters(18,45 °) using HiCamp image sequence II.s

PROJ	Frame	Estimated 2-D Hough Parameters (ρ, θ)			
		13.2dB	11.9dB	8.95dB	7.75dB
3	15	(18,47°)	(16,67°)	(22,67°)	(17,28°)
	20	(18,45°)	(18,45°)	(16,65°)	(22,67°)
	25	(18,45°)	(18,45°)	(18,45°)	(22,67°)
6	15	(18,47°)	(22,67°)	(22,67°)	(22,67°)
	20	(18,45°)	(19,47°)	(16,63)	(22,67°)
	25	(18,45°)	(18,45°)	(18,45°)	(17,69°)
9	15	(18,45°)	(16,63°)	(22,67°)	(22,678)
	20	(18,45°)	(18,45°)	(16,63°)	22,670°)
	25	(18,45°)	(18,45°)	(18,45°)	17,495°)

From the simulation results shown in the tables the accuracy of estimating the point target track parmaeters depends not only on the number or projections but on the signal-to-noise ratios and the number of time-sequential image data frames. Significantly, we could observe that there was not a large amount of residual increase in tracking performance then the number of projection is greater than six. For 2-D Hough parameter estimation of target tracks the proposed method could estimate the good porameters even under high noisy condi- tions. For some worst cases the good sets of track parameters ard obtained for the signal-to noise ratios down to 3.6 dBs. Comparing the resulte to those of the copressed tracj nao netgids [6][7][8], our approach is far up in the target trajeatory localization and estimation ability. From the simulation ran for those previously proposed methods the results show us that the single track map techniques could hardly detect and estimate target trajectory ρ arameters for the SNRs below 8 dBs, and the tracking performance degrades fast given the moderately high noisy data.

V. CONCLUSIONS

The focus of the paper has been on the track parameter estimation of the small, dim, moving tragets embedded in a sequence of digital infrared images. The simulation results have shown us that the performance of our genralized projection based Hough transform algorithm derived from Radon transform surpasses those of the traditional methods using the track map. Advantageously, for most of the cases the average of six projection frames was sufficed, and the tracking performance did not increase significantly when the number of projection frames exceeds six. For most of cases, the average of three projections taken along in parallel to three coordinate axes were adequate, but results also depended on the SNRs, the locations of the target track, and the number of target frames. In sum, our projection-based algorithm has performed robustly independent of image backgrounds.

Although there is an increase in the number of computation due to the number of projections taken, however, we could effectively use those overdetermined information in detecting and estimating the parameters of point target tracks much better than those of the traditional track map methods[6][7][8]. Furthermore, the implementation of the proposed algorithm is under investigation using GAPP (Geometric Arithmetic Parallel Processor, Martin Marietta Co.) and HPP(Hough transform processor, LSI Logic Co.) by exploiting the computational parallelism inherent in taking projections and the Hough transform. In addition, with the advent of fast and massive VLSI technology and optical processing methodology the hardware issues concer- ning real time processing become a trivial problem. Particularly, for the proposed scheme, the system needs on the average of 50Kbytes(32 X 32 X 50) of memory accomodating 50 data frames for the worst

case design. In actuality, the tracking system needs less than thirty frames, and it operates sequentially at the frame rate after the system initialization time of fifteen to twenty frame time delay. The issues concerning the real-time implementation is under research, and the results will be presented in later papars.

By far, the proposed generalized projection-based Hough transform algorithm is a novel approach in that the number of computations can be significantly reduced while processing the entrired 3 D volume of data as a whole and creathing a rubust detection and estimation entired ment even under highly noisy conditions. This makes 3 D target tracking problem be addressed at a real time possible. As a final remark, the extension of the proposed algorithm to the circular or the elliptical target trajectories is also under consideration.

REFERENCES

[1] P.V.C. Hough, Method and means for recognizing comples patterns, U. S. Patent 3069654, 1962/

[2] J. Illingworth and J. Kittler, "the adaptive Hough transform," IEEE Trans. on PAMI, vol. 9, no. 5, pp. 690-698, 1987.

[3] D.S. McKenzie and S.P. Protheroe, "Curve description using the invverse Hough transform," Pattern Recognition, vol. 23, pp. 283-290. 1990.

[4] W.E. Grimson and D.P. Huttenlocher, "On the sensitivity of the Hough transform for object recognition," IEEE Trans. on PAMI, pp. 275-282, 1990.

[5] C.C Hsu and J.S. Huang, "Partitioned Hough transform for ellipsoid detection," Pattern Recognition, vol. 23, no. 3/4, pp. 275-282. 1990.

[6] A.E. Cowart, W.E. Snyder, and W.H. Ruedger, "The detection of unresolved target using the Hough transform," CVGIP, vol, 21, pp. 222-238, 1983.

[7] M.L. Padgett, S.A. Rajala, W.E. Snyder, and W.H. Ruedger, "Use of the Hough transform for tracking maneuvering targets," Proceedings of SPIE, vol. 575. pp. 145-155, 1985.

[8] D. Casasent and R. Kirshnapuram, "Detection of target trajectories using the Hough tranform," Applied Optics, Vol. 26, no. 2, pp. 247-251, 1987.

[9] S.R. Deans, The Radon tranform and some of its applications, wiley, New York, 1983.

[10] P.L. Chu, "Optimal projection for multidimensional signal detection," IEEE Trans. on Assp, vol. 36, no. 5, pp. 755-786, 1988.

[11] Jae Ho Choi, "Projection-based transform method for estimating the tracks of point targets in image sequences," Ph.D. Thesis, NCSU, Raleigh, ND, USA, 1993.

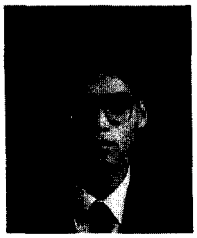

崔 在 虎 (Jea Ho Choi) 정회원
1963년 8월 14일생
1985년 5월 : NCSU(노스케롤라이나 주립대) 전기 및 컴퓨터 공학과 졸업
1988년 5월 : NCSU 전기 및 컴퓨터 공학과 공학석사
1993년 5월 : NCSU 전기 및 컴퓨터 공학과 컴퓨터 공학석사
1990년 1월 ~ 1993년 5월 : Research Triangle Institute. R.T.P., N.C., U.S.A. 시스템 공학 연구소 연구원
1994년 3월 ~ 현재 : 전북대학교 컴퓨터 공학과 전임강사
※주관심분야 : 다차원 신호처리, 영상통신, sensor fusion등

郭勳星(Hoon Sung Park) 정회원
1994년 6월 27일생
현재 : 전북대학교 컴퓨터 공학과 교수
제18권 제12호 참조